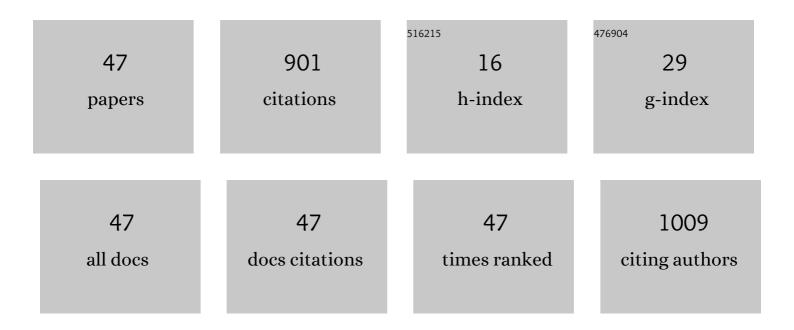
Wei-hau Chang

List of Publications by Year in descending order

Source: https://exaly.com/author-pdf/3646837/publications.pdf Version: 2024-02-01



#	Article	IF	CITATIONS
1	Activation of Prp28 ATPase by phosphorylated Npl3 at a critical step of spliceosome remodeling. Nature Communications, 2021, 12, 3082.	5.8	6
2	Copper Centers in the Cryo-EM Structure of Particulate Methane Monooxygenase Reveal the Catalytic Machinery of Methane Oxidation. Journal of the American Chemical Society, 2021, 143, 9922-9932.	6.6	36
3	Sub-3 Ã Cryo-EM Structures of Necrosis Virus Particles via the Use of Multipurpose TEM with Electron Counting Camera. International Journal of Molecular Sciences, 2021, 22, 6859.	1.8	2
4	rAMI – Rapid Alignment with Moment of Inertia for Cryo-EM Image Processing. Microscopy and Microanalysis, 2021, 27, 3216-3218.	0.2	0
5	Cryo-Ralib - A Modular Library for Accelerating Alignment in CRYO-EM. , 2021, , .		1
6	Catalytic machinery of methane oxidation in particulate methane monooxygenase (pMMO). Journal of Inorganic Biochemistry, 2021, 225, 111602.	1.5	7
7	Cryo-EM Analyses Permit Visualization of Structural Polymorphism of Biological Macromolecules. Frontiers in Bioinformatics, 2021, 1, .	1.0	5
8	NMR assignments of protrusion domain of capsid protein from dragon grouper nervous necrosis virus. Biomolecular NMR Assignments, 2020, 14, 63-66.	0.4	3
9	Pre-pro is a fast pre-processor for single-particle cryo-EM by enhancing 2D classification. Communications Biology, 2020, 3, 508.	2.0	12
10	XFEL coherent diffraction imaging for weakly scattering particles using heterodyne interference. AIP Advances, 2020, 10, .	0.6	9
11	Two-stage dimension reduction for noisy high-dimensional images and application to Cryogenic Electron Microscopy. Annals of Mathematical Sciences and Applications, 2020, 5, 283-316.	0.2	8
12	Characterization of a lytic vibriophage VP06 of Vibrio parahaemolyticus. Research in Microbiology, 2019, 170, 13-23.	1.0	24
13	Deriving a sub-nanomolar affinity peptide from TAP to enable smFRET analysis of RNA polymerase II complexes. Methods, 2019, 159-160, 59-69.	1.9	1
14	Development of a high-growth enterovirus 71 vaccine candidate inducing cross-reactive neutralizing antibody responses. Vaccine, 2018, 36, 1167-1173.	1.7	6
15	Free-electron-laser coherent diffraction images of individual drug-carrying liposome particles in solution. Nanoscale, 2018, 10, 2820-2824.	2.8	11
16	Conversion of a Peptide TAG to Sub-nanomolar Affinity for Single-Molecule Analysis of Protein Machinery. Biophysical Journal, 2018, 114, 565a.	0.2	0
17	The conserved AU dinucleotide at the 5′ end of nascent U1 snRNA is optimized for the interaction with nuclear cap-binding-complex. Nucleic Acids Research, 2017, 45, 9679-9693.	6.5	6
18	Zernike Cryo-EM with a Direct Electron Camera Enables Tracking Protein Conformations in the Temporal Dimension. Microscopy and Microanalysis, 2015, 21, 2145-2146.	0.2	1

Wei-hau Chang

#	Article	IF	CITATIONS
19	\$gamma\$-SUP: A clustering algorithm for cryo-electron microscopy images of asymmetric particles. Annals of Applied Statistics, 2014, 8, .	0.5	17
20	Hybrid electron microscopy-FRET imaging localizes the dynamical C-terminus of Tfg2 in RNA polymerase II–TFIIF with nanometer precision. Journal of Structural Biology, 2013, 184, 52-62.	1.3	10
21	Electron Microscopy-FRET Imaging Localizes the C-Terminus of the Second TFIIF Subunit in RNA Polymerase II-TFIIF with Nanometer Precision. Biophysical Journal, 2013, 104, 365a.	0.2	1
22	Zernike phase contrast cryo-electron microscopy reveals 100 kDa component in a protein complex. Journal Physics D: Applied Physics, 2013, 46, 494008.	1.3	8
23	Regulation of mammalian transcription by Gdown1 through a novel steric crosstalk revealed by cryo-EM. EMBO Journal, 2012, 31, 3575-3587.	3.5	26
24	Toward automated denoising of single molecular Fol^rster resonance energy transfer data. Journal of Biomedical Optics, 2012, 17, 011007.	1.4	5
25	A Lon-Like Protease with No ATP-Powered Unfolding Activity. PLoS ONE, 2012, 7, e40226.	1.1	13
26	Fabrication of influenza virus-like particles using M2 fusion proteins for imaging single viruses and designing vaccines. Vaccine, 2011, 29, 7163-7172.	1.7	22
27	Bioâ€Orthogonal Protein Labeling Methods for Single Molecule FRET. Journal of the Chinese Chemical Society, 2010, 57, 505-513.	0.8	1
28	A Single Molecule FRET Study of Formation of RNA Polymerase II Elongation Complex on Passivated Surface. Journal of the Chinese Chemical Society, 2010, 57, 514-521.	0.8	1
29	Fis-protein induces rod-like DNA bending. Chemical Physics Letters, 2010, 500, 318-322.	1.2	0
30	Roles of cysteines Cys115 and Cys201 in the assembly and thermostability of grouper betanodavirus particles. Virus Genes, 2010, 41, 73-80.	0.7	16
31	Zernike Phase Plate Cryoelectron Microscopy Facilitates Single Particle Analysis of Unstained Asymmetric Protein Complexes. Structure, 2010, 18, 17-27.	1.6	28
32	Mapping RNA exit channel on transcribing RNA polymerase II by FRET analysis. Proceedings of the National Academy of Sciences of the United States of America, 2009, 106, 127-132.	3.3	35
33	Phase TEM for biological imaging utilizing a Boersch electrostatic phase plate: theory and practice. Journal of Electron Microscopy, 2009, 58, 137-145.	0.9	30
34	Dibenzo[f,h]thieno[3,4-b] quinoxaline-Based Small Molecules for Efficient Bulk-Heterojunction Solar Cells. Organic Letters, 2009, 11, 4898-4901.	2.4	49
35	Role of the DxxDxD motif in the assembly and stability of betanodavirus particles. Archives of Virology, 2008, 153, 1633-1642.	0.9	30
36	Study of mean absorptive potential using Lenz model: Toward quantification of phase contrast from an electrostatic phase plate. Micron, 2008, 39, 749-756.	1.1	10

Wei-hau Chang

#	Article	IF	CITATIONS
37	Recent progresses in optical trap-and-stretch of red blood cells. , 2007, , .		3
38	Ubiquitin Ligase Activity of TFIIH and the Transcriptional Response to DNA Damage. Molecular Cell, 2005, 18, 237-243.	4.5	68
39	RNA Polymerase II/TFIIF Structure and Conserved Organization of the Initiation Complex. Molecular Cell, 2003, 12, 1003-1013.	4.5	86
40	Revised Subunit Structure of Yeast Transcription Factor IIH (TFIIH) and Reconciliation with Human TFIIH. Journal of Biological Chemistry, 2003, 278, 43897-43900.	1.6	35
41	Structure of Yeast RNA Polymerase II in Solution. Structure, 2002, 10, 1117-1125.	1.6	43
42	Point Mutagenesis and Cocrystallization of Wild-Type and Mutant Proteins:  A Study of Solid-Phase Coexistence in Two-Dimensional Protein Arrays. Langmuir, 2001, 17, 5731-5735.	1.6	7
43	Electron Crystal Structure of the Transcription Factor and DNA Repair Complex, Core TFIIH. Cell, 2000, 102, 609-613.	13.5	95
44	Electron Crystal Structure of an RNA Polymerase II Transcription Elongation Complex. Cell, 1999, 98, 791-798.	13.5	79
45	Electron crystallography of yeast RNA polymerase II preserved in vitreous ice. Ultramicroscopy, 1998, 70, 133-143.	0.8	10
46	The C-terminal Domain Revealed in the Structure of RNA Polymerase II. Journal of Molecular Biology, 1996, 258, 413-419.	2.0	35
47	Quantification of model bias underlying the phenomenon of Einstein from Noise. Statistica Sinica, 0, , .	0.2	0